Sigma J Eng & Nat Sci 38 (3), 2020, 1555-1566

Sigma Journal of Engineering and Natural Sciences
Sigma Mühendislik ve Fen Bilimleri Dergisi

**Research Article**

# LAMINAR FLOW OVER SLOPED DOWNSTREAM HEATED BOTTOM WALL BEHIND A BACKWARD-FACING STEP

**Seyfettin BAYRAKTAR*[1]**

[1]*Yildiz Technical University, Faculty Naval Architecture and Maritime, Department of Naval Architecture and Marine Engineering, İSTANBUL;* ORCID: 0000-0002-1554-353X

**Received: 07.11.2019 Revised: 25.05.2020 Accepted: 13.06.2020**

**ABSTRACT**

In the present three-dimensional study, laminar flow over a backward-facing step was investigated in the framework of the finite volume method for various Reynolds numbers ranging from 100 to 1000. Attempts were made to clarify the effects of the slope of the downstream heated bottom wall behind the step on the reattachment length and heat transfer. It was found that the length of the recirculation region changes slightly with the slope angles at lower Reynolds numbers while it changes dramatically as Reynolds number increases. The longest length of the recirculation region was obtained at the highest slope angle in the negative vertical-direction while the shortest one was determined at the maximum slope angle in the positive vertical direction. Increasing slope angles in both directions also provide a higher local Nusselt number in some distance behind the step.

**Keywords:** Backward-facing step, laminar flow, computational fluid dynamics, flow separation, reattachment length, heat transfer.

## 1. INTRODUCTION

Separation is a fluid flow phenomenon that occurs under various conditions. It is encountered in many engineering applications such as heat exchangers, nuclear reactors, power plants, heating and cooling devices, diffusers, airfoils, wind turbines, combustors, chemical processes and cooling passages in turbine blades, etc. The performance and efficiency of fluid machinery may greatly be influenced by the occurrence of the separation that also causes vibration and noise.

Due to the importance of flow separation in engineering systems, many studies have been done so far by means of a widely known case; the backward-facing step (BFS) flow. Flow over a BFS generates recirculation zones and forms vortices. These vortices occur due to the existence of the adverse pressure gradients in the fluid flow. The basic features of BFS flow are well known. A boundary layer which develops on a flat plate encounters BFS. The sudden change in surface geometry causes the boundary layer to separate at the sharp step edge. The resulting flow behaves like a free shear layer with a high-speed flow on the upper side and low-speed flow on the lower side. After some distance, the shear layer impinges on the surface and then forms a closed recirculation region containing moving fluid. Downstream of the reattachment the boundary layer

* Corresponding Author: e-mail: sbay@yildiz.edu.tr, tel: (212) 383 28 48

begins to redevelop. Studies involving BFS can be classified into two fundamental categories; experimental and numerical. Many numerical works were two-dimensional (2D) in the past due to the limited computing power and insufficient numerical techniques. Since the flow over BFS shows a 2D character in the range of Re=400 and Re=6000 [1], there is a vast number of studies in the literature that report 2D laminar [2], 2D turbulent and both 2D laminar and turbulent flows. Advances in computational fluid dynamics technique have enabled researchers to conduct realistic three-dimensional (3D) simulations than ever. It was reported that there are many parameters which affect the flow over BFS such as the inclination angle of the step [3], the shape of the step such as sharp or rounded [4], uncontrolled or controlled flows as well as normal or pulsed flows [5]. Flow over BFS has been investigated extensively due to its simplicity and applicability to heat transfer. It was reported that the reattachment causes a local augmentation of heat transfer. The maximum heat transfer coefficient is obtained upstream of the reattachment where turbulence intensity is high. Flow and heat transfer characteristics over modified BFS geometry have been taken into account by many researchers. A numerical study on heat transfer and flow over a baffle mounted onto the upper edge of a channel shows that as the baffle moves away from the step, the magnitude of the maximum Nusselt (Nu) number decreases [6]. Non-buoyant jet over BFS revealed that not only Re number but also Richardson (Ri) number and the oscillation frequency of the flow have profound effects on heat transfer [7]. Numerical investigation on the existence of obstacles in various shapes makes it clear that in term of the heat transfer the diamond-shaped obstacle is the best while the square shaped one is the worst [8]. In addition to the shape of the obstacle behind the step, the height of the obstacle also increases Nusselt number [9].

The cited studies show that many parameters that affect the heat transfer and fluid flow over the BFS with various configurations have been investigated. However, to the best of the author's knowledge, the inclination of the downstream bottom wall behind the BFS has not been investigated so far except [10] that reports the turbulent flow and heat transfer on an expanding channel. The main motivation of the present study is to reveal the effects of the inclination of the downstream bottom wall behind the BFS and effects of the inclination angle on the length of the recirculation region and heat transfer performance.

## 2. NUMERICAL METHOD

In the present study, Newtonian fluid with constant thermo-physical properties was assumed to flow over a BFS. A 3D computational domain consists of inlet and outlet channels was employed. The left side of the domain shown in Figure 1 was specified as the velocity inlet while the right side was set to pressure outlet. Effects of the inclination angle ($\alpha$) of the downstream bottom wall behind the step on the flow structure and heat transfer were investigated for three different angles in negative vertical-direction ($\alpha$=-1°, -2°, -3°) and two different angles in positive vertical-direction ($\alpha$=+1°, +2°) for three expansion ratios, ER=1.2500, 1.500 and 1.9423. The computational domain was set to cover the distance in x-direction $-30 \leq x/S \leq 50$ as recommended, [11]. The width of the channel was kept as B=35h [12]. The downstream bottom wall behind the step was subjected to constant wall temperature Tw=400 K while the remaining walls were assumed to be adiabatic. The temperature of the inlet fluid with constant properties was equal $T_\infty$=300 K. Flow was assumed to be fully laminar as explained below.

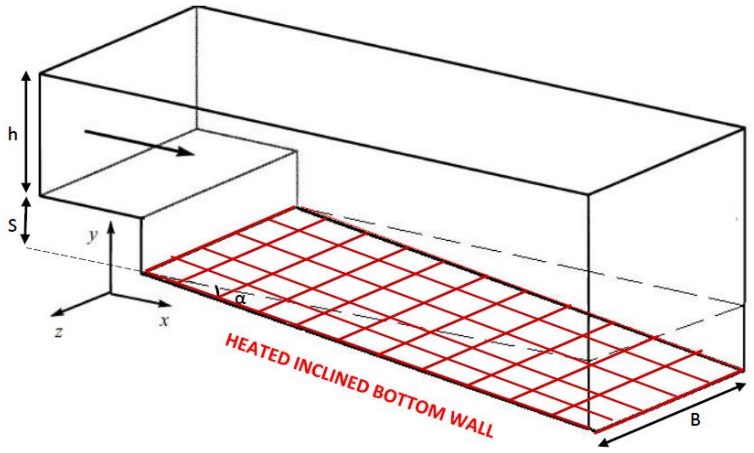


**Figure 1**. Sketch of the flow configuration for negative slope angle (α).

It was reported that the flow is laminar, transitional and turbulent for Re<1200, 1200<Re<6600 and Re>6600, respectively [1]. On the other hand, it was claimed that the transitional flow characteristics can be modeled by turbulence models such as Standard k-ε and RNG k-ε for the flows at Re=1000 specifically at further stations ( x/S>8) [13]. However, it was noted that some disagreements between the laminar and turbulent solutions may exist due to 2D domain. Actually, a previous work of [12] compromises the results of [1] and implies that the flow of BFS remains laminar for Re<1200. In the present study a 3D computational domain was used for flow at Re<1000 and hence it was assumed that the flow is laminar. The governing equations of the laminar flow are given below for continuity (Equation 1) and three components of momentum (Equation 2-Equation 4). The corresponding energy equation for incompressible, laminar flow with constant properties is given in Equation 5.

$$\frac{\partial u}{\partial x}+\frac{\partial v}{\partial y}+\frac{\partial w}{\partial z}=0 \tag{1}$$

$$\rho\left(u\frac{\partial u}{\partial x}+v\frac{\partial u}{\partial y}+w\frac{\partial u}{\partial z}\right)=-\frac{\partial p}{\partial x}+\mu\left(\frac{\partial^2 u}{\partial x^2}+\frac{\partial^2 u}{\partial y^2}+\frac{\partial^2 u}{\partial z^2}\right) \tag{2}$$

$$\rho\left(u\frac{\partial v}{\partial x}+v\frac{\partial v}{\partial y}+w\frac{\partial v}{\partial z}\right)=-\frac{\partial p}{\partial x}+\mu\left(\frac{\partial^2 v}{\partial x^2}+\frac{\partial^2 v}{\partial y^2}+\frac{\partial^2 v}{\partial z^2}\right) \tag{3}$$

$$\rho\left(u\frac{\partial w}{\partial x}+v\frac{\partial w}{\partial y}+w\frac{\partial w}{\partial z}\right)=-\frac{\partial p}{\partial x}+\mu\left(\frac{\partial^2 w}{\partial x^2}+\frac{\partial^2 w}{\partial y^2}+\frac{\partial^2 w}{\partial z^2}\right) \tag{4}$$

$$\left(u\frac{\partial T}{\partial x}+v\frac{\partial T}{\partial y}+w\frac{\partial T}{\partial z}\right)=\lambda\left(\frac{\partial^2 T}{\partial x^2}+\frac{\partial^2 T}{\partial y^2}+\frac{\partial^2 T}{\partial z^2}\right) \tag{5}$$

The above governing equations were discretized spatially on non-uniformly structured grids (Figure 2a). A special attention was paid to the regions where the upcoming flow detaches from the upstream wall and then reattaches to the bottom wall behind the step. Although grid elements with a smaller size generally ensure the high resolution of the flow field, there are some limitations such as the cost and time. Therefore, a mesh independence study was performed to guarantee that the results are grid independent. Five different meshes with 72000 (coarser mesh), 210000 (coarse mesh), 392000 (normal mesh), 632000 (fine mesh) and 1238000 (finer mesh) elements were tested in terms of the non-dimensional reattachment length ($X_R/S$). It was found that the reattachment length changes only 0.3% when the fine mesh was used instead of the normal mesh as shown in Figure 2b. Hence, all the simulations were done with normal mesh.

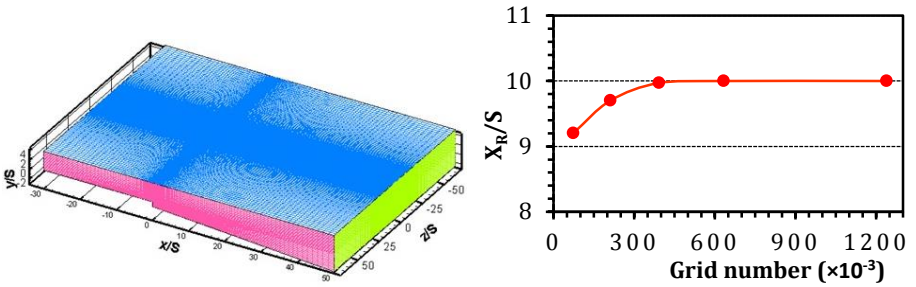


(a) (b)

**Figure 2.** Grid structure applied to the geometry, ER=1.25, α=-3° (a) and grid independence study at Re=500, ER=1.9423, α=0° (b).

The present study used the finite volume method to discretize the governing equations presented before using COUPLED scheme for pressure – velocity coupling. Second order and second order upwind schemes were utilized for pressure and momentum and energy equations, respectively. The simulations were performed on a laptop with 2.20 GHz CPU and 8 GB of RAM using CFD-based code Ansys Fluent. The flow Courant number was set 50 while the convergence criteria were set to $10^{-5}$ for the continuity and $10^{-6}$ for other equations.

## 3. RESULTS AND DISCUSSION

As noted in the previous section the flow was assumed to be laminar, hence it must be ensured that fully developed laminar velocity profiles are obtained before the step. It is also needed to show that the length before the step is sufficiently long for the parabolic velocity profile. Validations were achieved by comparing the results of the present study with the experimental data of [14], [15] and numerical results of [12]. It was shown that the streamwise velocity profile matches quite well with the theoretical solution and the experimental data (Figure 3a). Another comparison is presented in Figure 3b for ER=2.00 and Re=800. It is seen that at x/S=30 both results are in good agreement. Although the distribution of the streamwise velocity component at x/S=14 is very similar to that of [15] there are some discrepancies between both results at x/S=30 since this is a station close to the step where flow detaches and then recovers in a very complex flow field.

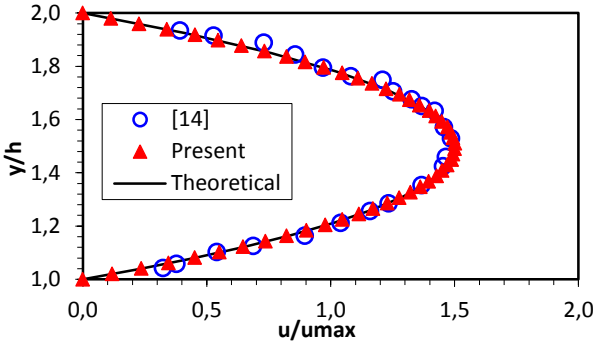


(a)

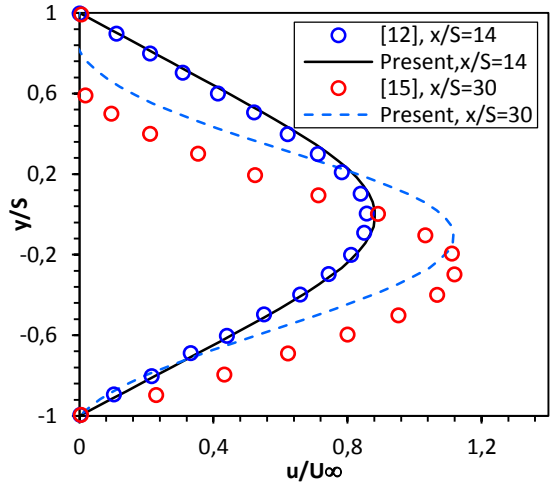


(b)

**Figure 3.** Comparison of the streamwise velocity component with data of a) Lee & Mateescu, 1998 [14] at x/S=-3.33, Re=500, ER=1.9423, $\alpha$=0° and b) Gartling, 1990 [15] at Re=800 and ER=2.00.

Reattachment length ($X_R$) is one of the most important characteristics of the flow over BFS and hence it has extensively been measured. Reattachment length is defined as the average distance from the step edge to the flow reattachment position. Obtained reattachment locations for ER=1.9423 were compared with the reattachment lengths found in the open literature as presented in Figure 4. It is seen that the results are in good agreement with the experimental data of [1] and numerical results of [16] - [19]. When Reynolds number increases the non-dimensional reattachment length deviates from the data of [16], [17] and [19] but still matches well with the data of [1] and [18].

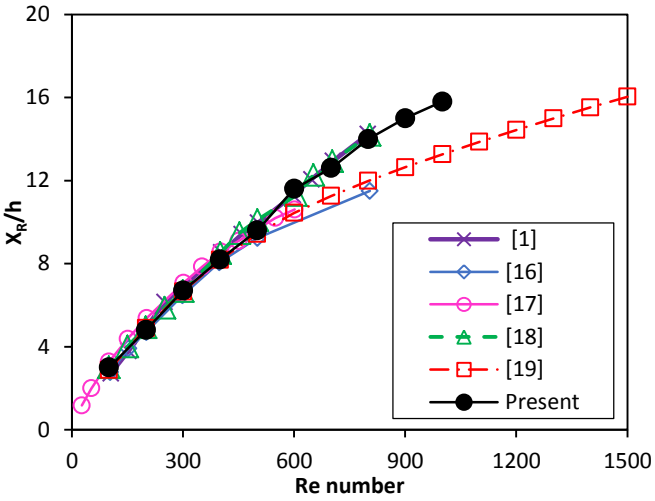


**Figure 4.** Comparisons of reattachment lengths versus Reynolds numbers, ER=1.9423.

The effects of the slope angle of the downstream heated bottom wall on the length of the recirculation zone are presented in Figure 5 for a wide range of Reynolds numbers. It is clear that the length of the recirculation region ($X_R$/s) changes slightly with the inclination angle in both negative and positive directions at low Reynolds numbers. Although the length of the recirculation region varies almost linearly with inclination angles for 100<Re<600 it changes curvilinearly with the inclination angle for Re≥600 due to the presence of the upper recirculation region seen at higher Reynolds numbers where the flow is retarded by viscous effects [16, 20]. The longest recirculation region is obtained at higher inclination angles in the negative vertical direction regardless of Reynolds number. Due to the shortened distance in the streamwise direction that enables fluid to recover the length of the recirculation region decreases with the increased inclination angles in the positive vertical direction. Since the lower Reynolds numbers cause to flow creeping over the surfaces behind the step the length of the recirculation region decreases with Reynolds numbers.

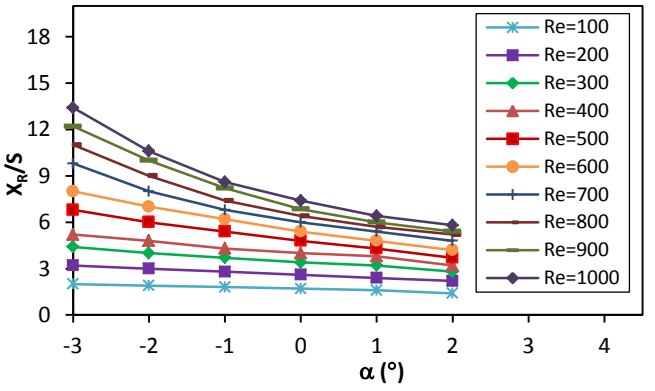


**Figure 5.** Effects of Re numbers and inclination angles of the downstream bottom wall after the step on the recirculation length ($X_R$/s) at ER=1.25.

Figure 6 presents that the length of the recirculation region increases with the inclination angle in the negative y-direction and decreases when the inclination angle of the downstream bottom wall behind the step increases in positive y-direction regardless of the expansion ratio (ER). Since an inverse proportion exists between the expansion ratio and length of the recirculation region the higher the expansion ratio the larger the length of the recirculation region. This is not surprising since higher expansion ratio implies high outlet channel due to the change of the inclination angle.

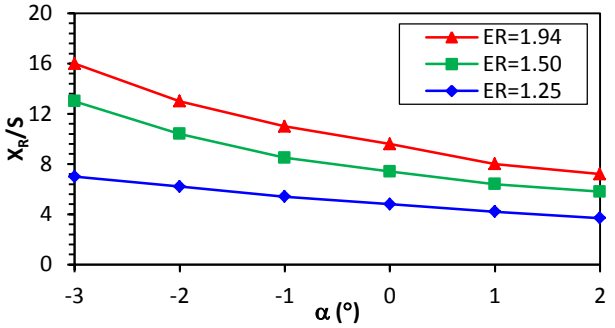


**Figure 6.** Effects of the ER on the reattachment length, Re=500.

Nusselt number distribution is plotted in Figure 7a versus the inclination angle of the downstream wall in the negative y-direction. It is noticed that Nusselt number suddenly increases due to flow of the fluid to the end of the recirculation region. As the downstream bottom wall behind the step is inclined further in the negative vertical-direction the magnitude of the peak Nusselt number increases due to the better heat transfer between the hot bottom wall and the fluid ($(Nu_{max})_{\alpha=0^\circ} < (Nu_{max})_{\alpha=-1^\circ} < (Nu_{max})_{\alpha=-2^\circ} < (Nu_{max})_{\alpha=-3^\circ}$). Since the length of the recirculation region increases with the inclination angle, the location of the peak Nusselt number is seen at x/S=10, x/S=11 and x/S=12 as the inclination angle in the negative vertical direction increases from $\alpha$=-1° to $\alpha$=-2° and $\alpha$=-3°, respectively. An increment in the slope angle in the positive vertical-direction provides a higher Nusselt number as in the negative vertical-direction (Figure 7a). The basic difference is that the peak Nusselt numbers for each slope angle are seen in very short distances compared to the negative vertical-direction due to the short length of the recirculation region. Effects of Reynolds number on the heat transfer are shown in Figure 7c for slope angle of $\alpha$=-3°. It reveals that the highest Nusselt number is obtained at the highest Reynolds number. As Reynolds number increases the peak values of Nusselt number are obtained at further streamwise directions.

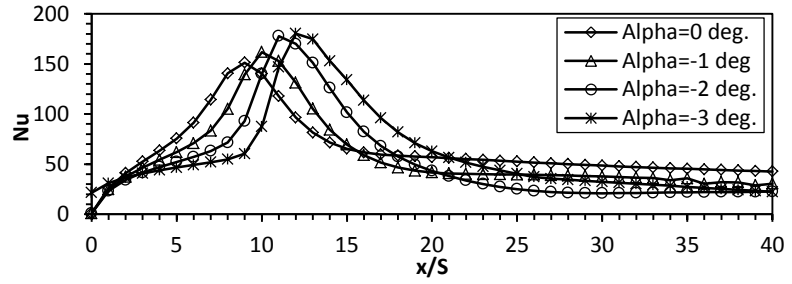


(a)

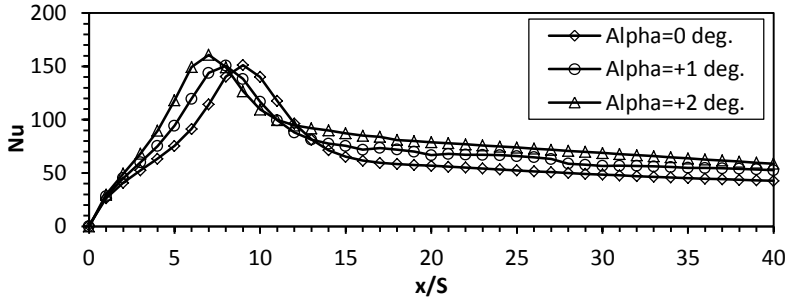


(b)

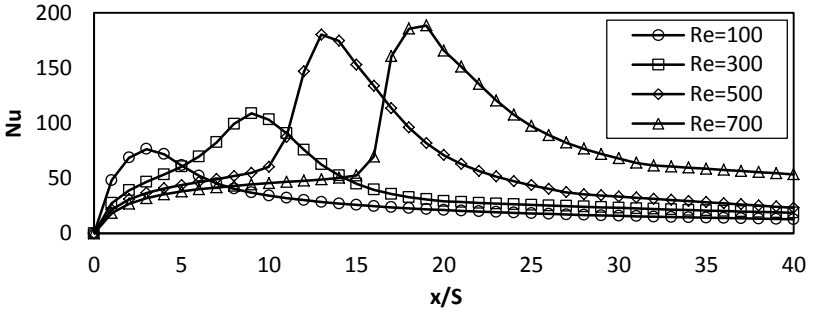


(c)

**Figure 7.** Change of Nu number with a) negative and b) positive slope angle of the downstream bottom wall, Re=500, c) Reynolds number, α=-3°.

As reported in the relevant literature, the main recirculation region forms behind the step on the bottom wall originates from the side wall and grows in size toward the center plane. It is seen in Figure 8 that the length of the recirculation region at the side wall is smaller than the size of the one in the symmetry plane. This conclusion is consistent with the literature that was reported for the straight bottom wall behind a BFS. It is also seen that when the slope angle decreases the length of the recirculation region on the bottom wall increases at first and an additional recirculation region occurs at the top wall that is formed at the symmetry plane at the same flow conditions. By the decreasing the slope angle the lengths of the recirculation regions increase and they grow in size as seen for α=-1°. Although not shown here, when the slope angle decreases further the flow region that contains mainly two large sized recirculation regions split into several flow regions due to the existence of more successive small sized recirculation regions. A foci is

seen near the top wall at x/S=18.2 while it is close to the bottom and moves to the upstream where the streamlines in the vicinity of that point spiral onto the bottom wall.

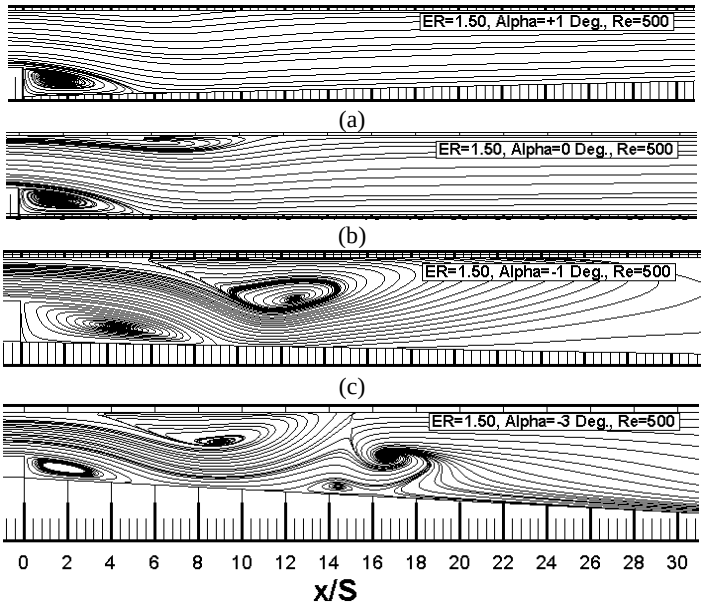


**Figure 8.** Effects of inclination angles on the flow field at the side walls, a) α=1°, b) α=0°, c) α=-1°, d) α=-3°, ER=1.50, Re=500.

Velocity profile distributions along the channel for various slope angles are presented in Figure 9 for Re=500. It is seen that slope angle does not become dominant factor on the velocity field until x/S=4. When the distance is doubled they start to differ from each other and the effect of the slope angle of the bottom wall is clearly seen at the last two stations. With respect to the horizontal direction it is seen that the velocity profile is not symmetric because flow accelerates as the bottom wall is sloped down in the negative y-direction.

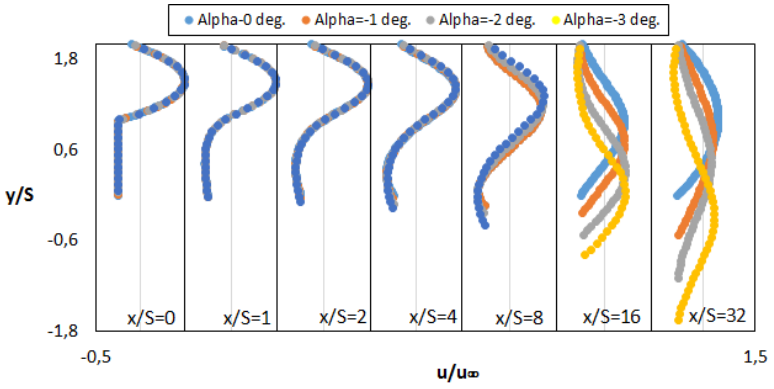


**Figure 9.** Velocity profiles for various slope angles of the bottom wall behind the step, Re=500.

Distributions of the friction coefficient (Cf) on the bottom wall behind the step are presented in Figure 10. Due to the buoyancy effects the sign of the skin friction coefficients do not change and whereas they change only in the positive y-direction. It is seen that as the slope angle of the bottom wall decreases the friction coefficient decreases as well.

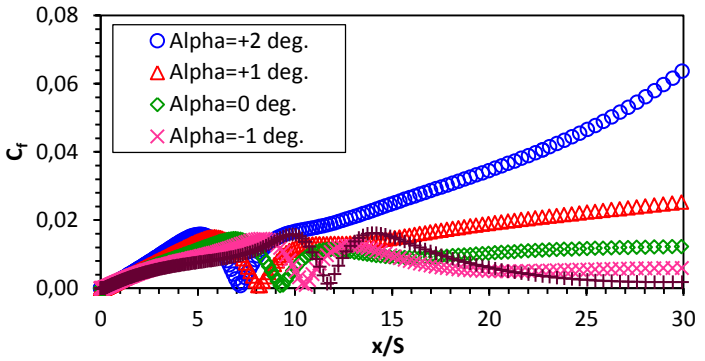


**Figure 10.** Skin friction coefficient ($C_f$) along the bottom wall, ER=1.9423, Re=500

## 4. CONCLUSION

The numerical results of laminar flow over a backward facing step located upstream of a sloped bottom wall are presented. Investigations on the effects of Reynolds number and expansion ratio on the reattachment length and heat transfer reveals that the reattachment length does not change with the inclination angle of the bottom wall behind the step at Re=100, however, it linearly changes with Reynolds number when the inclination angle is increased in the negative vertical-direction. For Re>600 length of the recirculation region increases as curvilinear with the inclination angle. It is seen that that there is a direct correlation between expansion ratio and the length of the recirculation region. Heat transfer between the hot inclined downstream bottom wall and the relatively cold fluid shows that Nusselt number increases with Re number as reported in conventional backward-facing step cases. Higher slope angles, both in negative and positive vertical directions provide highest Nusselt number.

## NOMENCLATURE

| | |
|---|---|
| B | Width of the channel (m) |
| BFS | Backward-facing step |
| $C_f$ | Friction coefficient |
| CFD | Computational Fluid Dynamics |
| ER | Expansion Ratio ($ER = \frac{h+S}{s}$) |
| h | Height of the inlet channel (m) |
| $k_f$ | Thermal conductivity of the fluid (W/mK) |
| Nu | Nusselt number $Nu = \frac{q_x S}{(T_w - T_b)k_f}$ |
| p | Pressure (N/m$^2$) |
| Re | Reynolds number $Re = \frac{u_\infty (2h)}{\nu}$ |
| Ri | Richardson number |
| $q_x$ | Wall heat flux (W/m$^2$) |
| S | Step height (m) |

| | |
|---|---|
| T | Temperature of the fluid (K) |
| $T_b$ | Bulk temperature (K) |
| $T_w$ | Wall temperature (K) |
| $T_\infty$ | Temperature of the inlet fluid (K) |
| u, v, w | Velocity components in x-, y- and z-directions, respectively (m/s) |
| x, y, z | Streamwise-, normal-, spanwise-direction |
| $X_R$ | Reattachment length (m) |
| 2D, 3D | Two-dimensional, three-dimensional |
| $\alpha$ | Inclination angle of the downstream bottom wall behind the step (°) |
| $\lambda$ | Thermal diffusivity of the fluid ($m^2/s$) |
| $\nu$ | Kinematic viscosity of the fluid ($m^2/s$) |
| $\mu$ | Dynamic viscosity of the fluid (kg/ms) |
| $\rho$ | Density of the fluid (kg/m) |

## REFERENCES


[1] Armaly, B.F., Durst, F., Pereire, J.C.F., Schonung, B., (1983) `Experimental and theoretical investigation of backward-facing step flow, *Journal of Fluid Mechanics* 127, 473-496.

[2] Batenko, S.R., Terekhov, V.I., (2002) Effect of Dynamic Prehistory on Aerodynamics of a Laminar Separated Flow in a Channel Behind a Rectangular Backward-Facing Step, *Journal of Applied Mechanics and Technical Physics* 43(6), 854-860.

[3] Bayraktar, S., (2014) Numerical solution of three-dimensional flow over angled backward-facing step with raised upper wall, *Journal of Applied Fluid Mechanics* 7(1), 155-167 (2014).

[4] Rygg, K., Alendal, G., Haugan, P.M., (2011) Flow over a rounded backward-facing step using a z-coordinate model and a σ-coordinate model, *Ocean Dynamics* 61, 1681-1696.

[5] Chuhn, K.B., Sung, H.J., (1996) Control of turbulent separated flow over a backward-facing step by local forcing, *Experiments in Fluids* 21, 417-426.

[6] Tsay, Y.L., Chang, T.S., Cheng, J.C. (2005) Heat transfer enhancement of backward-facing step flow in a channel by using baffle installation on the channel wall, *Acta Mechanica* 174, 63-76.

[7] Khanafer, K., Al-Azmi, B., Al-Shammari, A., Pop, I., (2008) Mixed convection analysis of laminar pulsating flow and heat transfer over a backward-facing step, *International Journal of Heat and Mass Transfer* 51, 5785-5793.

[8] Selimefendigil, F., Oztop, H., (2016) Numerical study of forced convection of nanofluid flow over a backward facing step with corrugated bottom wall in the presence of different shaped obstacles, *Heat Transfer Engineering* 37(15), 1280-1292.

[9] Togun, H., (2016) Laminar CuO-water nano-fluid flow and heat transfer in a backward-facing step with and without obstacle, *Applied Nanoscience* 6, 374-378.

[10] Terekhov, V.I., Bogatho, T.V., (2015) Aerodynamics and Heat Transfer in a Separated Flow in an Axisymmetric Diffuser with Sudden Expansion, *Journal of Applied Mechanics and Technical Physics*, 56(3), 471-478.

[11] Sheu, T.W.H., Rani, H.P., (2006) Exploration of vortex dynamics for transitional flows in a three-dimensional backward-facing step channel, *Journal of Fluid Mechanics* 550, 61-83.

[12] Chiang, T.P., Sheu. T.W.H., A. (1999) Numerical Revisit of Backward-Facing Step Flow Problem, *Physics of Fluids*, 11(4), 862-874.

[13] Gong, Y., Tanner, F.X., (2009) Comparison of RANS and LES Models in the Laminar Limit for a Flow over a Backward-Facing Step Using OpenFOAM, *9th International Multidimensional Engine Modeling Meeting at the SAE Congress*, April 2009, Detroit, Michigan, USA.

[14] Lee, T., Mateescu, D. (1998) Experimental and Numerical investigation of 2-D backward-facing step flow. *Journal of Fluids and Structures*; 12: 703-716.

[15] Gartling, D.K., (1990) A test problem for outflow boundary conditions-flow over a backward-facing step, *International Journal for Numerical Methods in Fluids* 11, 953-967.

[16] Barton, I.E., (1997) The entrance effect of laminar flow over a backward-facing step geometry, *International Journal for Numerical Methods in Fluids* 25, 633-644.

[17] Barber, R.W., Fonty, A., (2002) A numerical study of laminar flow over a confined backward-facing step using a novel viscous-splitting vortex algorithm, *In 4th GRACM Congress on Computational Mechanics*, 27-29 June 2002, Patras, Greece.

[18] Biswas, G., Breuer, M., Durst, F., (2004) Backward-facing step flows for various expansion ratios at low and moderate Reynolds numbers, *Journal of Fluids Engineering* 126, 362-374.

[19] Erturk, E., (2008) Numerical solutions of 2-d steady incompressible flow over a backward-facing step, part i: high Reynolds number solutions, *Computer and Fluids* 37, 633-655.

[20] Barton, I.E., (1994) Laminar flow past an enclosed and open backward-facing step, *Physics of Fluids A: Fluid Dynamics* 12, 4054-4056.